

Leveraging User-Diversity in Energy-Efficient Edge-Facilitated Collaborative Fog Computing

Antoine Paris, Hamed Mirghasemi, Ivan Stupia and Luc Vandendorpe

ICTEAM/ELEN/CoSy, UCLouvain, Louvain-la-Neuve, Belgium

Email: {antoine.paris, seyed.mirghasemi, ivan.stupia, luc.vandendorpe}@uclouvain.be

Abstract

With the increasing number of heterogeneous resource-constrained devices populating the current wireless ecosystem, enabling ubiquitous computing at the edge of the network requires moving part of the computing burden back to the edge to reduce user-side latency and relieve the backhaul network. Motivated by this challenge, this work investigates edge-facilitated collaborative fog-computing to augment the computing capabilities of individual devices while optimizing for energy-efficiency. Collaborative-computing is modeled using the Map-Reduce framework, consisting in two computing rounds and a communication round. The computing load is optimally distributed among devices, taking into account their diversity in terms of computing and communications capabilities. Devices local parameters such as CPU frequency and RF transmit power are also optimized for energy-efficiency. The corresponding optimization problem is shown to be convex and optimality conditions are obtained through Lagrange duality theory. A waterfilling-like interpretation for the size of the computing load assigned to each device is given. Numerical experiments demonstrate the benefits of the proposed collaborative-computing scheme over various other schemes in several respects. Most notably, the proposed scheme exhibits increased probability of successfully dealing with more demanding computations along with significant energy-efficiency gains. Both improvements come from the scheme ability to advantageously leverage devices diversity.

Index Terms

wireless collaborative computing, Map-Reduce, energy-efficiency, joint computation and communications optimization, fog computing.

I. INTRODUCTION

The current trends in communications and networking suggest that the future wireless ecosystem will be populated by a massive number of heterogeneous (in terms of computing

and communication capabilities) devices: from relatively powerful smartphones and laptops to ultra-low-power sensors, actuators and other connected “things” [1]. At the same time, emerging applications like virtual and augmented reality, context-aware computing, autonomous driving, Internet of Things (IoT) and so forth, require more and more computing capabilities while aiming for smaller and smaller latency. All in all, recent years have seen the focus moving from communications as an objective per se to communications as a way to enhance computing capabilities of energy limited devices [2], [3].

This paradigm shift started with Mobile Cloud Computing (MCC) [4] first, and with Multi-access Edge Computing (MEC) [5]–[7] later on. While MCC proved itself to be effective to enable ubiquitous computing on resource-constrained devices while prolonging their battery life, MEC has the advantage of offering smaller computing latency and reducing the pressure on the backhaul network. This makes MEC both more suitable for ultra-low-latency applications emerging from the recent 5G developments and more able to cope with the ever growing number of connected devices and their ever growing computing demand. Compared to MCC, the inherent spatial distribution of MEC also has the advantage of offering some level of decentralization.

In contexts where MCC latency is unacceptable and in the absence of MEC servers nearby or when the use of third-party owned MCC/MEC is deliberately ruled-out for privacy reasons, *fog computing* offers an even more decentralized alternative. Fog computing is formally defined in [8] as “*a huge number of heterogeneous wireless devices that **communicate and potentially cooperate among them and with the network** to perform processing tasks without the intervention of third parties*”. Those distributed computing resources can also be exploited to enhance the computing capabilities of *individual* devices. As MEC, fog computing benefits from reduced user-side latency and reduces the pressure on the backhaul network: two features recognized as key enablers for ubiquitous artificial intelligence (AI) at the edge of the network [9]. Achieving this, however, requires to move part of the computing burden from the powerful server-side to the resource-constrained user-side. To accommodate for relatively complex processing tasks on such limited devices requires to (i) enable devices collaboration to pool computing capabilities and (ii) take care of devices resources management, both in terms of computing resources and communications resources. It is also worth noting that fog computing can be integrated in a multi-tier architecture along with MEC and MCC [10]. In this paper, we jointly optimize for energy-efficiency the computation and communication resources of a set of heterogeneous and resources-constrained mobile devices taking part in collaborative fog computing.

A. Application scenario

As already mentioned, enabling computationally demanding intelligent mobile systems at the edge of the network requires to offload part of the computing burden to mobile devices to reduce user-side latency and relieve the backhaul network [9]. A recent comprehensive survey on “Deep Learning in Mobile and Wireless Networking” [11] discusses fog computing to support those two objectives in the context of machine learning (ML) or deep learning (DL) inference; two key components of ubiquitous AI. ML/DL models, however, often contain tens to hundreds of millions of parameters. As such, it might be prohibitive or even impossible for a single mobile device limited in computing, memory and battery capacity to process (or even store) the full ML/DL model needed to perform the inference with a reasonable latency [12]. Though it is possible to reduce the size of a ML/DL model using various model compression techniques such as pruning, weights quantization and so forth, this always comes at the cost of accuracy [13]. Enabling devices collaboration to augment their individual processing capabilities is another solution that does not sacrifice accuracy [12]. Combined with proper resources management and allocation to preserve devices battery life, this collaborative inference approach should allow the processing of reasonably large ML/DL models. It is worth noting that this kind of distributed/collaborative inference is envisioned as a key enabler to ubiquitous AI in future 6G networks [14]. This example application scenario, also known as “model-split” inference [15] and illustrated and detailed in Fig. 1, thus consists in distributing a ML/DL model pre-trained off-device in the cloud to perform collaborative on-device inferences on local input data later on.

B. Related works and motivations

This paper extends our previous work [16] with a more realistic energy consumption model and more degrees of freedom in the optimization of the collaborative-computing scheme. This new work can actually be particularized to our previous one (see Sec. V for comparison).

The system model used in this paper is inspired by previous works on wireless distributed computing (WDC) [17]–[22]. Most notably, we also use the Map-Reduce distributed computing framework [23] with an access point (AP) or base station (BS) facilitating the communications between devices (i.e., communications are *edge-facilitated*). The choice of Map-Reduce is also motivated by the example application of distributed/collaborative ML/DL inference [9], [14]. The vast majority of these works, however, study WDC from an information theoretic point of view, focusing on coded distributed computing (CDC) and discussing the trade-offs between the

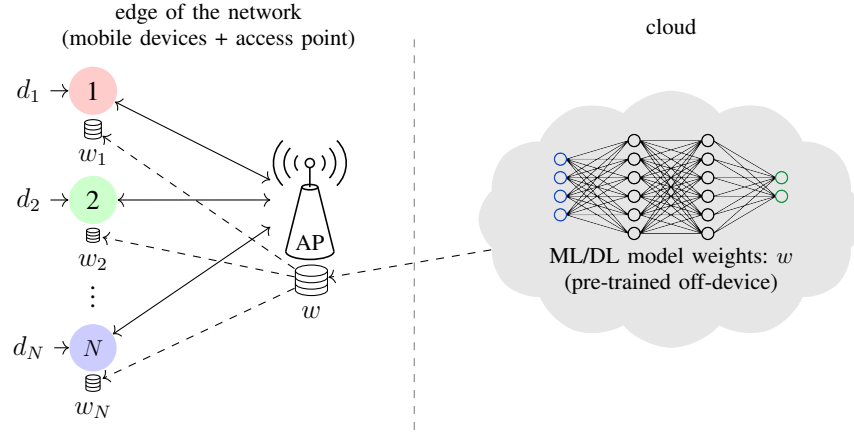


Fig. 1. Collaborative fog computing ML/DL inference scenario (adapted from the edge-based app-level mobile data analysis approach illustrated in [11]). The ML/DL model is first trained off-device in the cloud using offline datasets. The ML/DL model weights, noted w , are then offloaded to the edge of the network for future on-device inference. Each device $n \in [N]$ wants to perform some inference $\phi(d_n, w)$ on its local input data d_n using the model weights w . However, this operation might be prohibitive or even impossible to carry on a single mobile device due to memory, computing capabilities or battery limitations. Distributing the ML/DL model weights w across multiple devices to enable collaborative inference is envisioned as a potential solution to this issue [12]. It is also worth noting again that this fog computing inference scenario significantly reduces backhaul network traffic and user-side latency compared to the cloud-based scenario in which inferences are performed in the cloud [11].

computation and communication loads incurred by the collaboration. In short, the conclusion is that increasing devices computing load makes it possible to leverage network coding opportunities during the exchange of intermediate computation results, hence reducing the communication load. *Considering the inherent energy-limited nature of mobile devices as the main bottleneck to WDC, the focus in this work is shifted towards the allocation of computing and communication resources and optimization of the collaboration to minimize devices energy consumption.*

Most existing works on WDC consider the set of collaborating devices to be homogeneous in terms of computing and communication capabilities (with recent notable exceptions – still focused on CDC – like [18] and [22]). Under these conditions, the computing load is thus uniformly distributed across all devices. *Motivated by current trends in the wireless ecosystem, we here consider the set of devices to be heterogeneous instead.* As a consequence, it might no longer be optimal to uniformly distribute the computing load (e.g., the ML/DL model weights, see Fig. 1) across mobile devices. To allow our collaborative-computing scheme to take into account – and leverage – devices diversity, our model thus allows arbitrary partition of the computing load. Compared to previous works focused on CDC, we also make the latency constraint accompanying

the computing task an explicit constraint.

Various other cooperative-computing schemes were also studied in the literature, see e.g., [24]–[29]. [24] discusses cooperative-computing and cooperative communications in the context of MEC systems wherein a user can partially (or totally) offload a computing task to both a MEC server and a so-called helper device that can then (i) perform some local computations for the user device (i.e., cooperative computing), (ii) further offload part or all the task to the MEC server (i.e., cooperative communication), or (iii) both. The system model and problem formulation used in this work also owes a lot to [24], especially with regards to devices energy consumption models. [25] also devises an energy-efficient cooperative-computing scheme in which a mobile device can partially or totally offload a computing task to a surrounding idle device acting as a helper. In the context of Mobile Wireless Sensors Networks (MWSNs), [26] augments this framework by optimally selecting the helper device among a set of N surrounding devices. In [27], a wireless powered cooperative-computing scheme wherein a user device can offload computations to N helper devices is described. In [28] authors describe Mobile Device Cloud (MDC), i.e., a framework in which power balancing is performed among a cluster of mobile devices, and empirically optimize the collaboration to maximize the lifetime of the set of devices. Finally, in [29], an energy-efficient and incentive-aware network-assisted (i.e., coordinated by the edge of the network), device-to-device (D2D) collaboration framework is presented.

C. Objective and contributions

Given the heterogeneous nature of mobile devices and their limitations in terms of memory, computing capabilities and battery life, this work aims to provide insights into the following question: **how to distribute a computing load (e.g., ML/DL model) across an heterogeneous set of resource-constrained wireless devices to complete a given set of computing tasks (e.g., ML/DL inferences) in the most energy-efficient way, while satisfying a given deadline?**

More precisely, the contributions of this paper can be summarized as follows:

- we propose an N -devices edge-facilitated collaborative fog computing scheme based on the Map-Reduce distributed computing framework [23] and formulate a joint computation and communication resources optimization problem with energy-efficiency as objective ;
- we gain engineering insights into the structure of the optimal solution by leveraging Lagrange duality theory and offer a waterfilling-like interpretation for the size of the computing load assigned to each device ;

- through numerical experiments, we compare the performance of the proposed scheme with various other schemes using less degrees-of-freedom in the optimization (such as the one proposed in [16]) to analyze the relative benefits of each set of variables being optimized and to show that the proposed scheme advantageously exploits devices diversity.

D. Organization of the paper

Section II starts by describing in details the collaborative computing model and the energy and time consumption models for both local computation and edge-facilitated communications. Next, Sec. III formulates the joint computation and communication resources allocation problem and analyzes its feasibility. Section IV then reformulates the problem, proves its convexity in this new formulation and leverages Lagrange duality theory to gain some insights on the optimal solution of the problem. Section V benchmarks the performances of the optimal collaborative-computing scheme against various other schemes through numerical experiments. Finally, Sec. VI discusses the results obtained in this work, their limits, and opportunities for future research.

II. SYSTEM MODEL

As already illustrated in Fig. 1, we consider an heterogeneous set of N wireless devices indexed by $n \in [N]$ sharing a common AP or BS. Each device n wants to perform a given computing task $\phi(d_n, w)$ within a given latency τ , with d_n some D -bit local input data to device n and w some L -bit data common to all N devices. As detailed in Sec. I-A and in Fig. 1, w could be a ML/DL model that was pre-trained in the cloud, while $\phi(d_n, w)$ could represent an inference performed using this model w on an input d_n . Motivated by this example application, it is assumed that $L \gg D$. As a consequence of the large size of w , it might be impossible or prohibitive in terms of energy consumption for an *individual* device to complete the computing task $\phi(d_n, w)$ within the deadline τ . Devices thus pool together and collaborate to augment their individual computing capabilities. The collaborative computing model used in this work, i.e., Map-Reduce [23] is described in Sec. II-A. Next, and because we are here concerned by optimizing the energy-efficiency of the collaboration, Sec. II-B and II-C describe the models used to quantify the time needed and energy consumed by the different phases of the collaboration.

The AP/BS is responsible for coordinating and optimizing the collaboration. This makes our collaborative-computing scheme edge-facilitated (or network-assisted) and fits with the fog computing definition given in the introduction. To allow for offline optimization of the

collaborative-computing scheme, we assume that the AP/BS has perfect non-causal knowledge of the uplink channels (i.e., devices to AP/BS) during the communication phase, and perfect knowledge of the computing and communication capabilities of all devices. Although unrealistic with regard to the channels, this simplifying assumption allows us to provide a first performance evaluation of the proposed collaborative fog computing scheme in a best-case scenario.

A. Collaborative computing model

The computing tasks $\{\phi(d_n, w)\}_{n=1}^N$ (e.g., ML/DL inferences) are shared between N devices according to the Map-Reduce framework [23]. First, we assume that the L -bit data w (e.g., ML/DL model weights) can be arbitrarily partitioned in N smaller l_n -bit data w_n (one for each device n) with $l_n \in \mathbb{R}_{\geq 0}$ ¹ and

$$\sum_{n=1}^N l_n = L. \quad (1)$$

As opposed to previous works focusing on CDC [17]–[22], we are not assuming any redundancy in the computing loads $\{w_n\}_{n=1}^N$ assigned to each device, that is $w_i \cap w_j = \emptyset$ for all $i \neq j$. Also, the sizes $\{l_n\}_{n=1}^N$ of the assigned computing loads $\{w_n\}_{n=1}^N$ are optimized for energy-efficiency taking into account the diversity of devices instead of being uniform (e.g., $l_n = L/N$ or a multiple for all n) and fixed ahead of time. Assuming relatively large downlink rates, and because the focus is on the energy consumption of mobile devices (rather than the energy consumption of the AP), we neglect the time and energy needed to transmit w_n from the AP to device n , for all $n \in [N]$. To make collaborative-computing possible, we also assume that the D -bit local input data $\{d_n\}_{n=1}^N$ were shared between mobile devices through the AP in a prior phase that we neglect in this work because D is assumed to be relatively small compared to L [17], [18].

a) Map: During the first phase of the Map-Reduce framework, namely the *Map phase*, each device n produces intermediate computation results (e.g., partial inference results using a subset w_n of the ML/DL model weights w)

$$g_n(d_1, w_n), g_n(d_2, w_n), \dots, g_n(d_N, w_n)$$

where g_n is the *Map function* executed at device n . The size of the intermediate computation result $g_n(d_m, w_n)$ produced by device n for device m is assumed to be proportional to the size l_n

¹In practice, l_n should be an integer multiple of the size of the smallest possible division of w . In this work, we relax this practical consideration to avoid dealing with integer programming later on. Note that $l_n = 0$ is also possible, in which case device n **does not participate** to the collaboration.

of its assigned computing load w_n and is given by βl_n . Each device n thus computes intermediate computation results for all the other devices, i.e., $g_n(d_m, w_n)$ for all $m \neq n$, and for itself, i.e., $g_n(d_n, w_n)$, using the part w_n of w received from the AP. The Map phase is illustrated in the colored and framed columns of Fig. 2.

b) Shuffle: Next, devices exchange intermediate computation results with each other in the so-called *Shuffle phase*. As already mentioned multiple times, coded shuffling [17]–[22] is not considered in this work. In this simplified Shuffle phase, each device n thus directly transmits the intermediate computation results $g_n(d_m, w_n)$ to device m via the AP, for all $m \neq n$. Device n thus needs to transmit a total of $(N - 1)\beta l_n$ bits of intermediate computation results to the AP. To ease notations in the rest of the paper, we define $\alpha = (N - 1)\beta$. The Map phase can thus be seen as a data compression phase, reducing the size of w_n from l_n bits to αl_n bits of intermediate computation results before transmission in the Shuffle phase. The intermediate computation results exchanged during the Shuffle phase are indicated in bold on Fig. 2.

c) Reduce: Finally, during the *Reduce phase*, each device m combines a total of $\sum_{n=1}^N \beta l_n = \beta L$ bits of intermediate computation results $\{g_n(d_m, w_n)\}_{n=1}^N$ produced by all the collaborating devices as

$$\phi(d_m, w) = h_m(g_1(d_m, w_1), g_2(d_m, w_2), \dots, g_N(d_m, w_N))$$

where h_m is the *Reduce function* executed at device m . This last operation, which could be thought of as combining all the partial inference results produced by all the devices to get the final inference $\phi(d_m, w)$, is illustrated in the colored rows on Fig. 2.

We note t_n^{MAP} , t_n^{SHU} and t_n^{RED} the amount of time needed to perform the Map, Shuffle and Reduce phases, respectively, at device n . Because the Map and Shuffle phases must be over at every device before the Reduce phase starts (as all the intermediate computation results need to be available), we have the following constraint

$$t_n^{\text{MAP}} + t_n^{\text{SHU}} \leq \tau - \max_n \{t_n^{\text{RED}}\}, \quad n \in [N]. \quad (2)$$

B. Local computing model

During the Map phase, each device n receives l_n bits to process. The number of CPU cycles needed to process one bit of input data at device n is assumed to be given by a constant c_n . At the opposite of our previous work [16], devices are now assumed to be able to perform dynamic frequency scaling (DFS), i.e., a device can adjust its CPU frequency on the fly depending on the

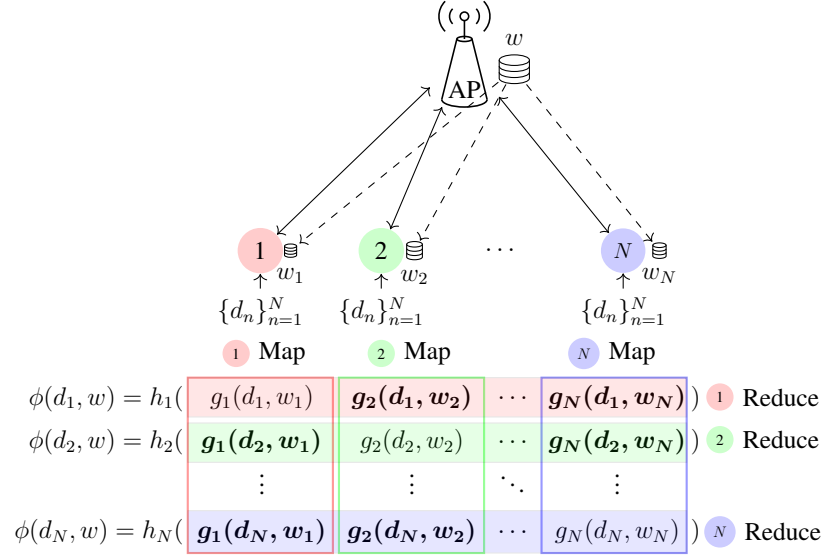


Fig. 2. Illustration of the Map-Reduce collaborative-computing model. The computing tasks $\{\phi(d_n, w)\}_{n=1}^N$ are shared across N devices. During the Map phase, each device n produces intermediate computation results $\{g_n(d_m, w_n)\}_{m=1}^N$ (see framed columns). Next, during the Shuffle phase, the intermediate computation results in bold on the figure are transmitted via the AP to the devices for which they have been computed. The AP is said to *facilitate* the communications. Finally, during the Reduce phase, each device m combines the intermediate values $\{g_n(d_m, w_n)\}_{n=1}^N$ to obtain $\phi(d_m, w)$ (see colored rows).

needs. Then, noting κ_n the effective capacitance coefficient (that depends on the chip architecture of each device), the energy needed for computation during the Map phase can be modeled as [6], [7], [24]

$$E_n^{\text{MAP}} = \frac{\kappa_n c_n^3 l_n^3}{(t_n^{\text{MAP}})^2}, \quad n \in [N] \quad (3)$$

with the following constraint

$$c_n l_n \leq t_n^{\text{MAP}} f_n^{\text{max}}, \quad n \in [N] \quad (4)$$

where f_n^{max} is the maximum CPU frequency of device n . Motivated by the fact that $D \ll L$ and to avoid integer variables in our optimization problem later on, the energy and time to process local input data $\{d_n\}_{n=1}^N$ during the Map phase have been neglected in both (3) and (4).

Similarly, the energy needed at device n to combine the βL bits of intermediate computation results during the Reduce phase can be modeled as

$$E_n^{\text{RED}} = \frac{\kappa_n c_n^3 (\beta L)^3}{(t_n^{\text{RED}})^2}, \quad n \in [N] \quad (5)$$

with the following constraint

$$c_n \beta L \leq t_n^{\text{RED}} f_n^{\text{max}}, \quad n \in [N]. \quad (6)$$

Because increasing t_n^{RED} is always favorable for energy-efficiency and because the Reduce phase cannot start before the Map and Shuffle phases are over, one can see that we will always have the same $t_n^{\text{RED}} = t^{\text{RED}}$ across all N devices. As a consequence, constraint (6) becomes

$$\beta L \max_n \left\{ \frac{c_n}{f_n^{\text{max}}} \right\} \leq t^{\text{RED}} \quad (7)$$

while constraint (2) becomes

$$t_n^{\text{MAP}} + t_n^{\text{SHU}} \leq \tau - t^{\text{RED}}, \quad n \in [N]. \quad (8)$$

C. Communications from the mobile devices to the AP

During the Shuffle phase, devices exchange intermediate computation results through the AP. This exchange thus involves both an uplink communication (devices to AP) and a downlink communication (AP to devices). In most applications however, it is reasonable to assume that the downlink rates are much larger than the uplink rates. For this reason, and because we are primarily interested by the energy consumed by the resource-constrained devices, we neglect the time needed for the downlink communications in this work.

We assume that all the devices can communicate in an orthogonal manner to the AP (e.g., through frequency division multiple access techniques, or through interference alignment [30]). Let h_n denote the wireless channel power gain from device n to the AP during the Shuffle phase, p_n the RF transmit power of device n , B the communication bandwidth and N_0 the noise power spectral density at the AP. The achievable uplink rate of device n is then given by²

$$r_n(p_n) = B \ln\left(1 + \frac{p_n h_n}{N_0 B}\right)$$

in nats/second³. Noting P_n^c the constant energy consumption of the communication circuits at device n , the energy consumed during the Shuffle phase is thus given by

$$E_n^{\text{SHU}} = t_n^{\text{SHU}}(p_n + P_n^c) \quad (9)$$

with the following constraints

$$\alpha l_n \leq t_n^{\text{SHU}} r_n(p_n), \quad n \in [N] \quad (10)$$

²The noise power $N_0 B$ can be multiplied by the SNR gap Γ to account for practical modulation and coding schemes. This additional factor is left out here for the sake of clarity.

³Nats and bits are used interchangeably in this paper (with the proper factor correction applied when needed) to avoid carrying $\ln(2)$ factors in the derivations later on.

and

$$p_n \leq p_n^{\max}, \quad n \in [N] \quad (11)$$

where p_n^{\max} is the maximum RF transmit power at device n .

III. PROBLEM FORMULATION

Putting everything together, the energy-efficient collaborative fog computing problem can be formulated as follows

$$\begin{aligned} \text{(P1)} : \quad & \underset{\mathbf{l}, \mathbf{t}^{\text{MAP}}, \mathbf{t}^{\text{SHU}}, \mathbf{t}^{\text{RED}}, \mathbf{p}}{\text{minimize}} && \sum_{n=1}^N E_n^{\text{MAP}} + E_n^{\text{SHU}} + E_n^{\text{RED}} \\ & \text{subject to} && (1), (4), (7), (8), (10), (11) \\ & && l_n, t_n^{\text{MAP}}, t_n^{\text{SHU}}, p_n, t_n^{\text{RED}} \geq 0, \quad n \in [N] \end{aligned}$$

where $\mathbf{l}, \mathbf{t}^{\text{MAP}}, \mathbf{t}^{\text{SHU}}$ and \mathbf{p} are N -length vectors containing the corresponding variables. Interestingly, this problem can be reformulated as follows: how can we send a total of L bits at a given rate of L/τ bits/second through N parallel special channels consisting of a ‘‘computing channel’’ in series with a wireless communication channel in the most energy-efficient way? This is illustrated in Fig. 3. This interpretation was already mentioned in [25] for a single channel (i.e., for $N = 1$) and is here generalized for multiple parallel channels.

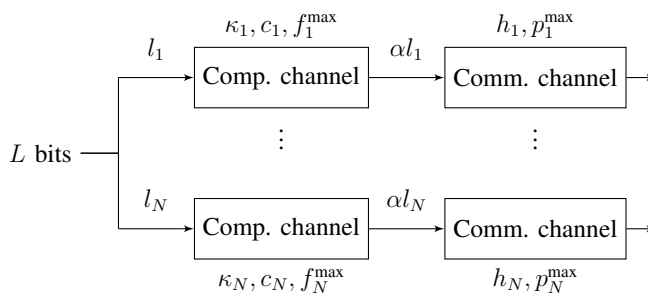


Fig. 3. Another interpretation of the energy-efficient collaborative fog computing problem: how can we send a total of L bits at a given rate of L/τ bits/second through N parallel special channels consisting of a ‘‘computing channel’’ in series with a wireless communication channel in the most energy-efficient way?

A. Feasibility

Before solving Problem (P1), we first seek to determine its feasibility condition, i.e., condition that ensures that the system is able to meet the deadline.

Lemma 1 (Feasibility). *Problem (P1) is feasible if and only if the task size L satisfies*

$$L \leq L_{\max} = \sum_{n=1}^N \frac{\tau - \beta L \max_n \left\{ \frac{c_n}{f_n^{\max}} \right\} f_n^{\max}}{1 + \frac{\alpha f_n^{\max}/c_n}{r_n(p_n^{\max})}} \frac{f_n^{\max}}{c_n}.$$

Proof. The maximum computing capacity of the system L_{\max} is obtained by solving the following optimization problem

$$\begin{aligned} L_{\max} \triangleq & \underset{l, t^{\text{MAP}}, t^{\text{SHU}}, t^{\text{RED}}, p}{\text{maximize}} && \sum_{n=1}^N l_n \\ & \text{subject to} && (4), (7), (8), (10), (11) \\ & && l_n, t_n^{\text{MAP}}, t_n^{\text{SHU}}, p_n, t^{\text{RED}} \geq 0 \quad \forall n. \end{aligned}$$

For the maximum computing capacity to be achieved, constraints (8), (11) and (7) must be met, that is, the entire time τ is used by all devices, all devices transmit at their maximum RF transmit power p^{\max} and the Reduce phase executes as fast as possible. Next, the two constraints (4) and (10) on l_n can be re-written in a single constraint as follows

$$l_n \leq \min \left\{ \frac{t_n^{\text{MAP}} f_n^{\max}}{c_n}, \frac{1}{\alpha} t_n^{\text{SHU}} r_n(p_n^{\max}) \right\}.$$

At the optimum, this constraint is satisfied and, given the relationship between t_n^{MAP} and t_n^{SHU} , we have

$$\alpha \frac{t_n^{\text{MAP}} f_n^{\max}}{c_n} = t_n^{\text{SHU}} r_n(p_n^{\max})$$

which intuitively means that the number of bits of intermediate values produced by the Map phase at full speed must equal the number of bits that can be transmitted at full speed during the Shuffle phase. Then using the satisfied constraints (8) and (7) together, we have

$$t_n^{\text{MAP}} + t_n^{\text{SHU}} = \tau - \beta L \max_n \left\{ \frac{c_n}{f_n^{\max}} \right\},$$

which allows us to finally obtain

$$t_n^{\text{MAP}} = \frac{\tau - \beta L \max_n \left\{ \frac{c_n}{f_n^{\max}} \right\}}{1 + \frac{\alpha f_n^{\max}/c_n}{r_n(p_n^{\max})}} \quad \text{and} \quad t_n^{\text{SHU}} = \frac{\tau - \beta L \max_n \left\{ \frac{c_n}{f_n^{\max}} \right\}}{1 + \frac{r_n(p_n^{\max})}{\alpha f_n^{\max}/c_n}}. \quad (12)$$

The maximum computing load L_{\max} is thus given by

$$L_{\max} = \sum_{n=1}^N \frac{\tau - \beta L \max_n \left\{ \frac{c_n}{f_n^{\max}} \right\} f_n^{\max}}{1 + \frac{\alpha f_n^{\max}/c_n}{r_n(p_n^{\max})}} \frac{f_n^{\max}}{c_n}.$$

□

We see through (12) that, at full capacity, the time for the Map and Shuffle phases is shared according to the ratio of (i) the maximum rate at which the Map phase can produce intermediate computation results $\alpha f_n^{\max}/c_n$, and (ii) the maximum rate at which the Shuffle phase can transmit intermediate computation results $r_n(p_n^{\max})$. At lower than full capacity, these time intervals will be able to adjust taking into account the energy-efficiency of both phases.

IV. OPTIMAL SOLUTION

Inspired by [24], we then introduce a new set of variables $E_n = t_n^{\text{SHU}} p_n$, i.e., the RF energy consumed by the Shuffle phase, and substitute p_n for E_n/t_n^{SHU} to convexify Problem (P1). With this new variable, constraints (10) and (11) can be re-written as

$$\alpha l_n \leq t_n^{\text{SHU}} r_n \left(\frac{E_n}{t_n^{\text{SHU}}} \right) \quad (13)$$

and

$$E_n \leq t_n^{\text{SHU}} p_n^{\max} \quad (14)$$

respectively, for all $n \in [N]$. Problem (P1) thus becomes

$$\begin{aligned} \text{(P2)} : \quad & \underset{l, t^{\text{MAP}}, t^{\text{SHU}}, t^{\text{RED}}, E}{\text{minimize}} && \sum_{n=1}^N \frac{\kappa_n c_n^3 l_n^3}{(t_n^{\text{MAP}})^2} + E_n + t_n^{\text{SHU}} P_n^c + \frac{\kappa_n c_n^3 (\beta L)^3}{(t_n^{\text{RED}})^2} \\ & \text{subject to} && (1), (4), (7), (8), (13), (14) \\ & && l_n, t_n^{\text{MAP}}, t_n^{\text{SHU}}, E_n, t_n^{\text{RED}} \geq 0 \quad n \in [N]. \end{aligned}$$

We now prove the convexity of this new formulation.

Lemma 2 (Convexity). *Problem (P2) is convex.*

Proof. As this is a minimization problem, we start by showing the convexity of the objective function. The function x^3 is a convex function for $x \geq 0$. Its perspective function, x^3/y^2 , is thus also a convex function for $y > 0$. The term associated to the energy consumed by the Map phase is thus jointly convex with respect to $l_n \geq 0$ and $t_n^{\text{MAP}} > 0$. Next, the terms associated to the energy consumed by the Shuffle phase are linear and hence convex by definition. Finally, the function $1/x^2$ is a convex function with respect to $x > 0$ which makes the term associated to the energy consumed by the Reduce phase a convex function as well. As convexity is preserved under addition, the objective function of Problem (P2) is a convex function. We then show that the set defined by the constraints is a convex set. The equality constraint (1) is affine and thus defines a hyperplane. Next, inequalities (4), (7), (8), and (14) are either linear or affine and thus

define a polyhedron. The only remaining constraint (omitting trivial positivity constraints on all variables) is then constraint (13). For constraint (13) to define a convex set, its right-hand side term must be a concave function. The function $r_n(x)$ is a concave function with respect to $x \geq 0$. Its perspective function, $yr_n(x/y)$ is thus also a concave function with respect to $x \geq 0$ and $y > 0$. Because the intersection of a hyperplane, a polyhedron and a convex sublevel set remains a convex set, the set defined by the constraints of Problem (P2) is also convex. \square

Problem (P2) can easily be solved using a software for convex optimization like `cvxopt` [31]. This wouldn't however offer any interpretation of the results. To this effect, we seek to gain some insights into the optimal solution to Problem (P2) mathematically using Lagrange duality theory.

We thus let $\lambda \in \mathbb{R}$, $\beta_n \geq 0$, $\mu_n \geq 0$ be the Lagrange multipliers associated with constraints (1), (8) and (13) respectively. The partial Lagrangian is then given by

$$\begin{aligned} \mathcal{L}(\mathbf{x}, \boldsymbol{\mu}, \boldsymbol{\beta}, \lambda) &= \sum_{n=1}^N \frac{\kappa_n c_n^3 l_n^3}{(t_n^{\text{MAP}})^2} + E_n + t_n^{\text{SHU}} P_n^c + \frac{\kappa_n c_n^3 (\beta L)^3}{(t_n^{\text{RED}})^2} \\ &\quad + \sum_{n=1}^N \mu_n \left(\alpha l_n - t_n^{\text{SHU}} r_n \left(\frac{E_n}{t_n^{\text{SHU}}} \right) \right) \\ &\quad + \beta_n (t_n^{\text{MAP}} + t_n^{\text{SHU}} + t_n^{\text{RED}} - \tau) \\ &\quad + \lambda \left(L - \sum_{n=1}^N l_n \right) \end{aligned}$$

where optimization variables and Lagrange multipliers have been aggregated in the corresponding vectors to ease notations. The dual function is then given by

$$\begin{aligned} \text{(DF)} : \quad g(\boldsymbol{\mu}, \boldsymbol{\beta}, \lambda) &= \min_{\mathbf{x}} \quad \mathcal{L}(\mathbf{x}, \boldsymbol{\mu}, \boldsymbol{\beta}, \lambda) \\ &\text{s.t.} \quad (4), (7), (14) \\ &\quad 0 \leq t_n^{\text{MAP}}, t_n^{\text{SHU}}, t_n^{\text{RED}} \leq \tau \quad n \in [N], \\ &\quad l_n, E_n \geq 0 \quad n \in [N]. \end{aligned}$$

As the dual function provides a lower bound to the optimal value of the primal problem, we then seek to maximize it to obtain the best possible lower bound. The dual problem is given by

$$\begin{aligned} \text{(D1)} : \quad &\underset{\boldsymbol{\mu}, \boldsymbol{\beta}, \lambda}{\text{maximize}} \quad g(\boldsymbol{\mu}, \boldsymbol{\beta}, \lambda) \\ &\text{subject to} \quad \mu_n, \beta_n \geq 0, \quad n \in [N]. \end{aligned}$$

Problem (P2) is convex (Lemma 2) and satisfies Slater's condition if it is strictly feasible (in the sense given in Lemma 1). Strong duality thus holds and Problem (P2) can be solved by solving the dual problem (D1).

A. Derivation of the dual function

Before solving the dual problem (D1), we seek to evaluate the dual function $g(\boldsymbol{\mu}, \boldsymbol{\beta}, \boldsymbol{\lambda})$ for all $\boldsymbol{\mu}, \boldsymbol{\beta}, \boldsymbol{\lambda}$ by solving Problem (DF). To this effect, we first decompose Problem (DF) in $2N + 1$ sub-problems as follows

$$\begin{aligned} & \underset{l_n, t_n^{\text{MAP}}}{\text{minimize}} && \frac{\kappa_n c_n^3 l_n^3}{(t_n^{\text{MAP}})^2} + (\alpha \mu_n - \lambda) l_n + \beta_n t_n^{\text{MAP}} \\ & \text{subject to} && 0 \leq l_n \leq t_n^{\text{MAP}} f_n^{\text{max}} / c_n \\ & && t_n^{\text{MAP}} \leq \tau \end{aligned} \quad (15)$$

$$\begin{aligned} & \underset{E_n, t_n^{\text{SHU}}}{\text{minimize}} && E_n + (P_n^c + \beta_n) t_n^{\text{SHU}} - \mu_n t_n^{\text{SHU}} r_n \left(\frac{E_n}{t_n^{\text{SHU}}} \right) \\ & \text{subject to} && 0 \leq E_n \leq t_n^{\text{SHU}} p_n^{\text{max}} \\ & && t_n^{\text{SHU}} \leq \tau \end{aligned} \quad (16)$$

$$\begin{aligned} & \underset{t^{\text{RED}}}{\text{minimize}} && \sum_{n=1}^N \frac{\kappa_n c_n^3 (\beta L)^3}{(t^{\text{RED}})^2} + \beta_n t^{\text{RED}} \\ & \text{subject to} && \beta L \max_n \left\{ \frac{c_n}{f_n^{\text{max}}} \right\} \leq t^{\text{RED}} \leq \tau. \end{aligned} \quad (17)$$

It is interesting to note that Problems (15) and (16) correspond to the Map and Shuffle phases at device n respectively while Problem (17) corresponds to the Reduce phase.

Lemma 3 (Solution of Problem (15)). *For any $\mu_n, \beta_n \geq 0$ and $\lambda \in \mathbb{R}$, the optimal solution of Problem (15) satisfies*

$$l_n^* = M_n^* t_n^{\text{MAP}*} \quad (18)$$

with M_n^* , the effective processing rate (in bits/second) of device n defined as

$$M_n^* \triangleq \begin{cases} 0 & \lambda - \alpha \mu_n \leq 0 \\ \sqrt{\frac{\lambda - \alpha \mu_n}{3 \kappa_n c_n^3}} & \lambda - \alpha \mu_n \in]0, 3 \kappa_n c_n (f_n^{\text{max}})^2[\\ \frac{f_n^{\text{max}}}{c_n} & \lambda - \alpha \mu_n \geq 3 \kappa_n c_n (f_n^{\text{max}})^2 \end{cases} \quad (19)$$

and $t_n^{\text{MAP}*}$ given by

$$t_n^{\text{MAP}*} \begin{cases} = 0 & \rho_{1,n} < 0 \\ \in [0, \tau] & \rho_{1,n} = 0 \\ = \tau & \rho_{1,n} > 0 \end{cases} \quad (20)$$

with $\rho_{1,n} = 2\kappa_n(c_n M_n^*)^3 - \beta_n + \gamma_{2,n} \frac{f_n^{\max}}{c_n}$ and

$$\gamma_{2,n} = \begin{cases} 0 & M_n^* < \frac{f_n^{\max}}{c_n} \\ \lambda - \alpha\mu_n - 3\kappa_n c_n (f_n^{\max})^2 & M_n^* = \frac{f_n^{\max}}{c_n}. \end{cases} \quad (21)$$

Proof. See Appendix A. □

Lemma 4 (Solution of Problem (16)). *For any $\mu_n, \beta_n \geq 0$, the optimal solution of Problem (16) satisfies*

$$E_n^* = p_n^* t_n^{SHU*} \quad (22)$$

with p_n^* , the RF transmit power used during the Shuffle phase at device n defined as

$$p_n^* \triangleq \begin{cases} 0 & B\mu_n \leq \frac{BN_0}{h_n} \\ B\left(\mu_n - \frac{N_0}{h_n}\right) & B\mu_n \in \left[\frac{BN_0}{h_n}, \frac{BN_0}{h_n} + p_n^{\max}\right] \\ p_n^{\max} & B\mu_n \geq \frac{BN_0}{h_n} + p_n^{\max} \end{cases} \quad (23)$$

and t_n^{SHU*} given by

$$t_n^{SHU*} \begin{cases} = 0 & \rho_{2,n} < 0 \\ \in [0, \tau] & \rho_{2,n} = 0 \\ = \tau & \rho_{2,n} > 0 \end{cases} \quad (24)$$

with $\rho_{2,n} = \mu_n r_n(p_n^*) - P_n^c - \beta_n - \mu_n \frac{p_n^* \frac{h_n}{N_0}}{1 + p_n^* \frac{h_n}{N_0 B}} + \delta_{2,n} p_n^{\max}$ and

$$\delta_{2,n} = \begin{cases} 0 & p_n^* < p_n^{\max} \\ \mu_n \frac{\frac{h_n}{N_0}}{1 + p_n^{\max} \frac{h_n}{N_0 B}} - 1 & p_n^* = p_n^{\max}. \end{cases} \quad (25)$$

Proof. See Appendix B. □

Lemma 5 (Solution of Problem (17)). *For any $\beta_1, \dots, \beta_N \geq 0$, the optimal solution of Problem (17) satisfies*

$$t^{RED*} = \begin{cases} \beta L \max_n \left\{ \frac{c_n}{f_n^{\max}} \right\} & \sum_{n=1}^N \beta_n > \frac{2 \sum_{n=1}^N \kappa_n c_n^3}{\left(\max_n \left\{ \frac{c_n}{f_n^{\max}} \right\} \right)^3} \\ \beta L \sqrt[3]{\frac{2 \sum_{n=1}^N \kappa_n c_n^3}{\sum_{n=1}^N \beta_n}} & \sum_{n=1}^N \beta_n \leq \frac{2 \sum_{n=1}^N \kappa_n c_n^3}{\left(\max_n \left\{ \frac{c_n}{f_n^{\max}} \right\} \right)^3}. \end{cases} \quad (26)$$

Proof. See Appendix C. □

B. Maximization of the dual function and interpretation

The dual function being concave but non-differentiable, we could now maximize it using the subgradient-based ellipsoid method, as was done for example in [24]. However, in addition to being unpractical to solve the actual problem (when compared to the use of a convex optimization solver like `cvxopt` [31]), this method doesn't offer any additional insight into the structure of the optimal solution.

Instead, we intuitively look at what happens if we maximize the dual function $g(\boldsymbol{\mu}, \boldsymbol{\beta}, \lambda)$ taking into account the results of Lemmas 3, 4 and 5. To ease the analysis, we start with $\lambda = 0$ and $\mu_n = 0$ for all n . In this case, $l_n^* = 0$ for all devices and the penalty term $L - \sum_{n=1}^N l_n^* = L$ associated with λ appearing in the dual function is strictly positive. Intuitively, this implies that the task has not been fully distributed across the devices, violating constraint (1). It is thus possible to increase the value of the dual function through this positive penalty term by increasing the value of λ . Because l_n^* is proportional to $\sqrt{\lambda - \alpha\mu_n}$ through M_n^* , this increases the number of bits l_n^* processed by each device. Moreover, because l_n^* is also inversely proportional to $\sqrt{\kappa_n c_n^3}$ through M_n^* , less energy-efficient devices (i.e., the ones with larger values of $\kappa_n c_n^3$) get fewer bits to process. The value of λ can be increased in this way until the penalty term $L - \sum_{n=1}^N l_n^*$ equals 0 (i.e., until the task is fully distributed across the devices). Next, because $\mu_n = 0$ for all devices as of now, the penalty term $\alpha l_n^* - t_n^{\text{SHU}^*} r_n(p_n^*) = \alpha l_n^*$ associated with μ_n appearing in the dual function is strictly positive for all devices. Intuitively, this implies that the rate constraint (13) is violated for all devices. It is thus possible to increase the value of the dual function through this penalty term by increasing the value of μ_n . Increasing μ_n has a double effect: (i) it decreases the value of l_n^* because l_n^* is proportional to $\sqrt{\lambda - \alpha\mu_n}$, and (ii) it increases the value of p_n^* because p_n^* is directly proportional to μ_n . Combined, these two effects work together towards satisfying the rate constraint (13). For devices with very bad channel or very low maximum RF transmit power p_n^{\max} , μ_n could increase so much that $\lambda - \alpha\mu_n$ would become negative, meaning that the number of bits to be processed l_n^* would fall to 0. At this point, there is an iterative interplay between λ and $\{\mu_n\}_{n=1}^N$ in which both successively increase to maximize the dual function until both constraints (1) and (13) are satisfied and a maximum has been reached.

It is now possible to give a waterfilling-like interpretation of the structure of the optimal computing load partition $\{l_n^*\}_{n=1}^N$. First, λ acts as a kind of global (i.e., across all devices) water level for $\{l_n^*\}_{n=1}^N$ through the effective processing rate M_n^* . Then, $\alpha\mu_n$ can be seen as the base

of the water vessel of device n . Following the above discussion, this base $\alpha\mu_n$ mainly depends on the communication capabilities of device n (i.e., h_n and p_n^{\max}). Finally, the actual water content of each vessel, i.e., $\lambda - \alpha\mu_n$ is divided by $3\kappa_n c_n^3$. This term, related to the computing energy-efficiency of device n can be interpreted as a pressure applied to the water vessel of each device. The less energy-efficient device n is, the larger $3\kappa_n c_n^3$ becomes and the more pressure is applied to its water vessel, hence reducing the corresponding water level and l_n^* .

V. NUMERICAL RESULTS

In this section, the performances of the optimal collaborative-computing scheme (denoted Opt in what follows) are benchmarked against various other schemes through numerical experiments. The schemes used for comparison are

- **Blind**: the task allocation (i.e., choosing the value of l_n for each device n) doesn't take into account the heterogeneity of the devices; the scheme is blind to device diversity (both in terms of computing and communicating capabilities). In this case, the variable l_n is set to L/N for each device n . This corresponds to what is done in most works on CDC assuming homogeneous devices [17], [19], [20].
- **NoDFS**: the CPU frequency of each device n is fixed to its maximum value f_n^{\max} rather than being optimized for energy-efficiency. In this case, the variable t_n^{MAP} is set to $c_n l_n / f_n^{\max}$ for each device n while t_n^{RED} (now different for each device) is set to $c_n \beta L / f_n^{\max}$. This scheme is close to the one proposed in our previous work [16].
- **Blind-NoDFS**: this scheme combines the two previous cases. In this case, $l_n = L/N$ and $t_n^{\text{MAP}} = \frac{c_n}{f_n^{\max}} \frac{L}{N}$ for each device n while $t_n^{\text{RED}} = c_n \beta L / f_n^{\max}$. The only optimization left here concerns the Shuffle phase and the variables t_n^{SHU} and E_n .
- **NoOpt**: in this scheme, nothing is optimized. This is basically **Blind-NoDFS** with $\alpha \frac{L}{N} = t_n^{\text{SHU}} r_n \left(\frac{E_n}{t_n^{\text{SHU}}} \right)$ and $E_n = t_n^{\text{SHU}} p_n^{\max}$.

The parameters used in the following numerical experiments are given in Table I [6], [7], [24].

A. Maximum computing load and outage probability

To show that the proposed scheme indeed enhances the computing capabilities of individual devices, we start by comparing the maximum computing load of Opt and **Blind**, noted L_{\max}^{Opt} and L_{\max}^{Blind} , respectively. Other schemes are not included here as $L_{\max}^{\text{NoDFS}} = L_{\max}^{\text{Opt}}$ and

TABLE I
PARAMETERS USED IN THE NUMERICAL EXPERIMENTS.

Parameter	Value	Units
κ_n	$\overset{\text{i.i.d.}}{\sim} \text{Unif}([10^{-28}, 10^{-27}])$	/
c_n	$\overset{\text{i.i.d.}}{\sim} \text{Unif}([500, 1500])$	[CPU cycles/bit]
f_n^{\max}	$\overset{\text{i.i.d.}}{\sim} \text{Unif}([1, 3])$	[GHz]
h_n	$\overset{\text{i.i.d.}}{\sim} \mathcal{CN}(0, 10^{-3})$ (Rayleigh fading)	/
p_n^{\max}	$\overset{\text{i.i.d.}}{\sim} \text{Unif}([10, 25])$	[mW]
P_n^c	$\overset{\text{i.i.d.}}{\sim} \text{Unif}([10, 25])$	[mW]
B	15	[kHz]
N_0	1	[nW/Hz]

$L_{\max}^{\text{Blind-NoDFS}} = L_{\max}^{\text{Blind}} = L_{\max}^{\text{NoOpt}}$. For Opt, the maximum computing load L_{\max}^{Opt} can be readily obtained using Lemma 1. For Blind, we introduce the following Lemma.

Lemma 6 (Maximum computing load of Blind). *The maximum computing load achievable by the Blind scheme is given by*

$$L_{\max}^{\text{Blind}} = N \min \left\{ \frac{\tau - \beta L \max_n \left\{ \frac{c_n}{f_n^{\max}} \right\} f_n^{\max}}{1 + \frac{\alpha f_n^{\max} / c_n}{r_n(p_n^{\max})}} \frac{f_n^{\max}}{c_n} \right\}.$$

Proof. Obtaining L_{\max}^{Blind} requires solving the following linear program

$$\begin{aligned} L_{\max}^{\text{Blind}} \triangleq & \underset{l, t_n^{\text{MAP}}, t_n^{\text{SHU}}}{\text{maximize}} && Nl \\ & \text{subject to} && c_n l \leq t_n^{\text{MAP}} f_n^{\max} && \forall n \\ & && \alpha l \leq t_n^{\text{SHU}} r_n(p_n^{\max}) && \forall n \\ & && t^{\text{RED}} \geq \beta L \max_n \left\{ \frac{c_n}{f_n^{\max}} \right\} \\ & && t_n^{\text{MAP}} + t_n^{\text{SHU}} \leq \tau - t^{\text{RED}} && \forall n \\ & && l, t_n^{\text{MAP}}, t_n^{\text{SHU}} \geq 0 && \forall n \end{aligned}$$

A reasoning similar to the one used in Lemma 1 – and omitted here for the sake of space – can then be used to obtain the analytical expression given above. \square

Values of L_{\max}^{Opt} and L_{\max}^{Blind} for different values of the allowed latency τ and various numbers of devices N are plotted in Fig. 4. As expected, both L_{\max}^{Opt} and L_{\max}^{Blind} grow with the allowed

latency τ . However, L_{\max}^{Opt} grows with τ much faster than L_{\max}^{Blind} does. Next, one can see that increasing the number of devices N for a given allowed latency τ is always more profitable for `Opt` than for `Blind`. Furthermore, the benefits of further increasing the number of devices N remain constant for `Opt` but quickly saturates for `Blind`. Both observations can be explained by the fact that `Opt` is able to leverage devices diversity by optimally exploiting the different computing and communicating capabilities of the devices while `Blind`, as per its name, is not.

Another way of looking at the maximum computing loads of the different schemes is through what we define as the “outage probability” of the system. In this context, the outage probability is defined, for a random heterogeneous set of devices and a given allowed latency τ , as the probability that the maximum computing load that can be processed by the system is lower than the actual computing load L , i.e.,

$$P_{\text{out}}^* = \Pr [L \geq L_{\max}^*].$$

For a given task size L , this probability can be empirically computed by averaging over a large number of randomly generated sets of devices. For $L = 10$ Mb, both $P_{\text{out}}^{\text{Opt}}$ and $P_{\text{out}}^{\text{Blind}}$ are depicted in Fig. 5 as a function of the allowed latency τ and for several values of N . This plot again demonstrates the benefits of leveraging devices diversity to distribute the task among the devices. At the opposite, we see that `Blind` suffers from devices diversity. Indeed, for larger values of the allowed latency τ , increasing the number of devices N penalizes `Blind` by increasing its outage probability $P_{\text{out}}^{\text{Blind}}$. Intuitively, this comes from the fact that increasing the number of devices N increases the probability of having a very weak device limiting the whole system. Mathematically, the lower tail of the distribution of L_{\max}^{Blind} grows larger and larger with N , making the distribution more and more skewed towards small values of L_{\max}^{Blind} . This also explains why this trend was not visible on Fig. 4 as it only shows the mean of the distribution of L_{\max}^{Blind} . In addition, it appears that the benefits on $P_{\text{out}}^{\text{Blind}}$ of allowing a looser deadline (for a given N) saturate as the value of τ increases beyond a certain point that varies with the number of devices N . Again, and for the same reason, this trend was not visible on Fig. 4 and cannot be explained by looking at the mean of L_{\max}^{Blind} only. This saturation effect appears when the mode of the distribution of L_{\max}^{Blind} becomes larger than the value of the actual computing load L used to compute $P_{\text{out}}^{\text{Blind}}$. Passed this point, the benefits on $P_{\text{out}}^{\text{Blind}}$ of further pushing the mode to larger values by increasing τ become smaller and smaller.

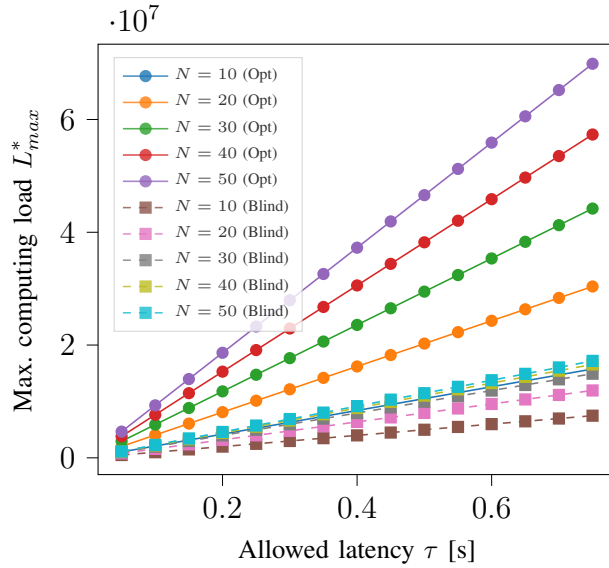


Fig. 4. Maximum computing loads L_{max}^{Opt} and L_{max}^{Blind} averaged over 1.000.000 random instances of the problem. Note that L_{max}^{Opt} for $N = 10$ is hidden by L_{max}^{Blind} for $N = 30, 40$ and 50 .

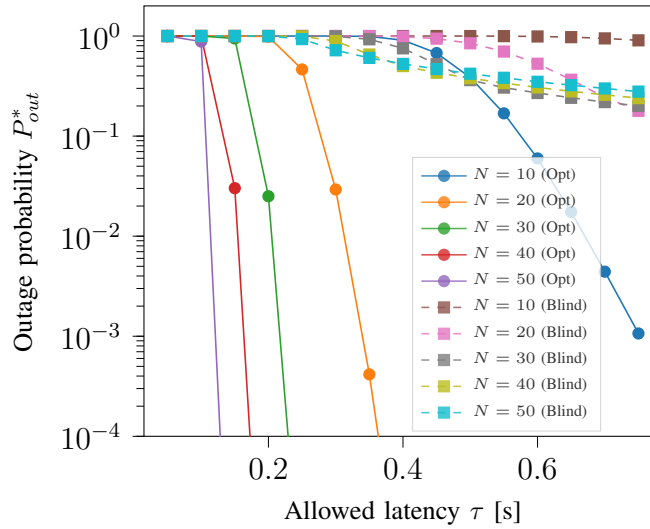


Fig. 5. Empirical outage probability P_{out}^{Opt} and P_{out}^{Blind} for $L = 10$ Mb, averaged over 1.000.000 random instances of the problem.

Coming back to the example application of collaborative on-device ML/DL inference, this indicates that Opt enables inferences with larger ML/DL models (i.e., more accurate/complex inferences) for the same latency, or the other way around, similar inferences for a smaller latency.

B. Energy consumption

We now look at the energy consumed by the different collaborative-computing schemes. Fig. 6a depicts the total energy consumed per bit processed for different numbers of devices N , while Fig. 6b depicts the energy consumed by each phase of the collaboration (i.e., Map, Shuffle and Reduce). First, one can observe that the energy consumed by both `Blind-NoDFS` and `NoOpt` is actually the same. This stems from the fact that it is always optimal (from an energy-efficiency point of view) for constraint (13) to be met. Indeed, the opposite would mean that the device is investing either too much time t_n^{SHU} (hence increasing the energy consumption of the communications circuits $t_n^{\text{SHU}} P_n^c$) or too much RF energy E_n with regards to the number of bits αl_n that needs to be transmitted in the Shuffle phase. For the same reason, constraint (14) is almost always satisfied as well, meaning that devices participating to the Shuffle phase transmit at the maximum RF power allowed, i.e., p_n^{max} . Schemes `Blind-NoDFS` and `NoOpt` are thus equivalent and both transmit at the maximum RF transmit power and at the maximum rate. These two observations are valid for all the other schemes as well. In addition, the energy per bit consumed by both `Blind-NoDFS` and `NoOpt` is roughly constant with the number of devices. At the opposite, the energy consumed by the other schemes decreases with N as diversity across the devices is exploited for energy-efficiency. Interestingly, optimizing $\{t_n^{\text{MAP}}\}_{n=1}^N$ and t^{RED} only (in `Blind`) is more beneficial than optimizing l_n only (in `NoDFS`), even though the number of bits assigned to each device for processing by `Blind` is uniform across the devices, and thus blind to diversity. Combining both schemes in `Opt` leads to a gain in energy-efficiency with respect to `NoOpt` reaching two orders of magnitude for large values of N .

Fig. 6b breaks down the energy consumption of the different schemes in 3 components: E^{MAP} , E^{SHU} and E^{RED} . Note that `NoOpt`, being equivalent to `Blind-NoDFS`, has been omitted to avoid cluttering the plot. First, it appears that the energy consumption of the Map phase largely dominates the energy consumption of the Shuffle and Reduce phases for small values of N^4 . As the number of devices N increases, this difference decreases for all schemes leveraging diversity across the devices (i.e., all but `Blind-NoDFS`). At the opposite, the energy consumed by the Shuffle phase increases with the number of devices N , no matter the scheme used. This figure

⁴Note that this statement is strongly dependent on the energy consumption model and the parameters used for the numerical experiments. As an example, increasing the number of bits transmitted during the Shuffle phase, αl_n , through the total size of the intermediate computation results βL would directly result in an increase of E^{SHU} by the same factor.

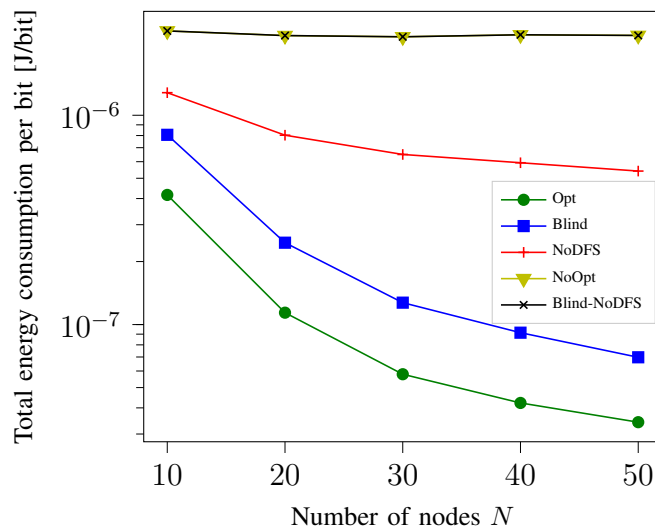
also shows that there is not much (if anything) to gain from optimization in the Shuffle phase. Next, one can see that the energy efficiency of the Reduce phase increases with N when t^{RED} can be optimized (i.e., when devices can perform DFS). This decrease with N is however slower than what we observed for the Map phase. For `Blind`, this can be explained by the fact that priority in the optimization is given to the more energy intensive Map phase. For `Opt`, this comes from the fact that, at the opposite of the Map phase, all devices have to perform the Reduce phase. Finally, for `NoDFS` and `Blind-NoDFS`, each device has to perform the Reduce phase at full speed causing E^{RED} to increase with N .

C. Energy-latency trade-off

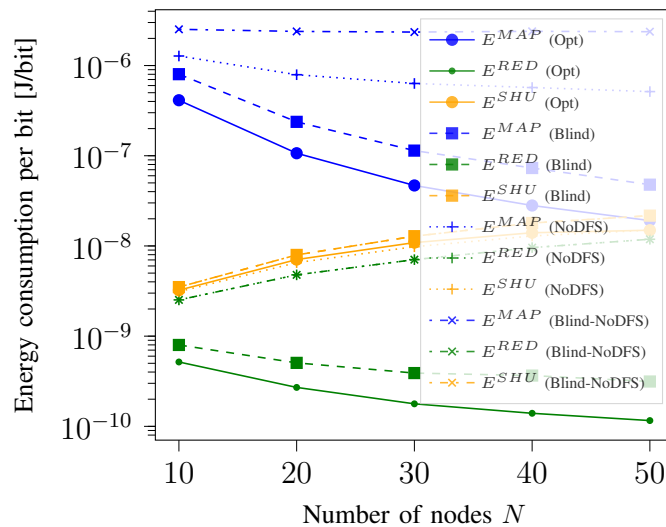
Fig. 8 depicts the total energy consumption per bit and the energy consumed per bit by each phase for the different schemes and for different values of the allowed latency τ . Interestingly, Fig. 8 closely resembles Fig. 6, implying that the effect of increasing the number of devices N is roughly equivalent to the effect of increasing the allowed latency τ . The underlying mechanisms, however, are different. For schemes where devices are able to perform DFS (i.e., `Opt` and `Blind`), increasing τ enables the devices to further decrease their CPU frequency, hence saving energy. For `NoDFS`, increasing τ enables the system to increase the number of bits assigned to the most energy-efficient devices, hence reducing the load on less energy-efficient devices and again saving energy.

D. Number of participating devices

Finally, Fig. 7 shows the average fraction of devices participating to the collaboration, i.e., devices with $l_n > 0$ that thus participate to the Map and Shuffle phases, as a function of the computing load L/L_{max} . For `Blind` (and `Blind-NoDFS`), this fraction is of course constant and equal to 1 as $l_n = L/N$ for all n . For `Opt`, this fraction starts at around 0.6 for very small computing loads and quickly reaches 1 for computing loads > 0.2 . At the opposite, for `NoDFS`, the fraction of devices participating to the Map and Shuffles phases closely follows the fraction L/L_{max} . To explain these radically different behaviors, we look at the energy consumed by the Map phase at each device n for both schemes. For `Opt` first, Eq. (3) indicates that E_n^{MAP} is a cubic function of l_n . For `NoDFS`, injecting $t_n^{\text{MAP}} = c_n l_n / f_n^{\text{max}}$ in (3) shows that E_n^{MAP} becomes a linear function of l_n . This explains why the computing load is more evenly spread across devices for `Opt` than for `NoDFS`.



(a) Comparison of the total energy consumed by the different schemes as a function of the number of devices N . Note that the energy consumption is the same for both NoOpt (yellow curve) and Blind-NoDFS (black curve).



(b) Breakdown of the energy consumed by the three phases of the collaboration as a function of the number of nodes N . Note that the energy consumption for the Reduce phase is the same for both NoDFS and Blind-NoDFS.

Fig. 6. Energy consumption of the devices for $L = 1$ Mb, $\beta L = 0.1$ kb and $\tau = 100$ ms as a function of the number of devices N . Each point is the result of an average over 100 feasible (for each scheme) instances of the problem, i.e., instances for which $L \leq L_{\max}^{\text{Opt}}, L_{\max}^{\text{Blind}}$. Note that the parameters have also been chosen to allow comparison between the schemes, i.e., to ensure that feasible instances arise with reasonable probability for all schemes.

VI. DISCUSSION AND FUTURE WORKS

This work built upon our previous work [16] to further highlight the benefits of leveraging devices diversity – whether in terms of computing or communication capabilities – to enhance individual computing capabilities of the devices while increasing energy-efficiency of the system as a whole. As mentioned in the introduction, this makes collaborative-computing another potential viable architecture to be used in conjunction with MEC and MCC to enable ubiquitous computing on heterogeneous devices. However, further validation with more realistic and practical assumptions is needed. Interferences between devices during the Shuffle phase, for example, were neglected in this work. As the interference level is expected to increase with the number of devices participating to the Shuffle phase, taking into account interference in the communication model could have a significant impact on the number of devices participating to the collaboration. Non-causal knowledge of the uplink channels was also assumed to allow for offline optimization of the collaboration. To get rid of this unrealistic assumption, one could instead consider the expectation taken over the channel gain h_n of $r_n(p_n)$ in constraint (10) for a given channel gain distribution. Adaptation to the actual channel condition observed during the Shuffle phase could then be performed on-the-fly by each device. Downlink communications were also neglected in this work. While this makes sense in a scenario where optimizing the energy-consumption of

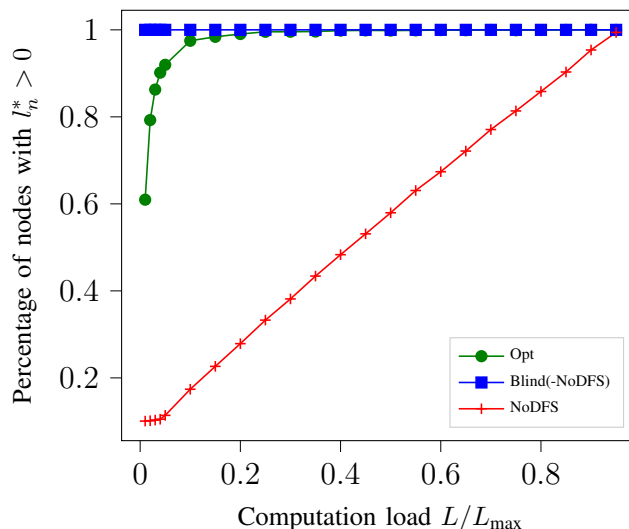
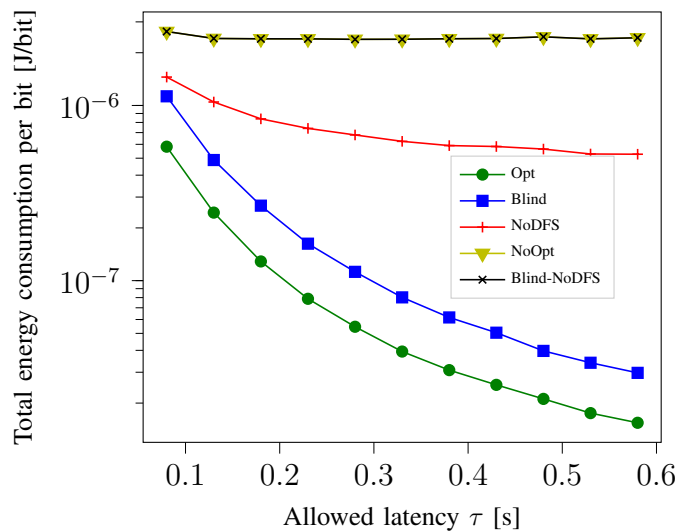
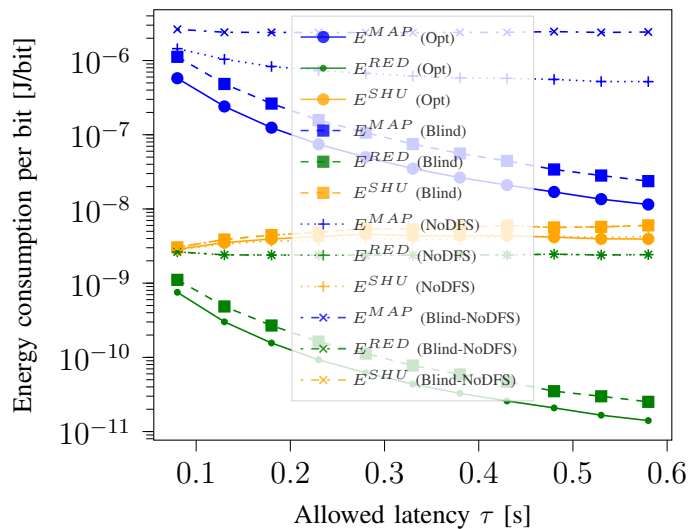


Fig. 7. Average fraction of devices participating to the collaboration, i.e., devices with $l_n^* > 0$ that thus participate to the Map and Shuffle phases, as a function of the computing load L/L_{\max} .



(a) Comparison of the total energy consumed by the different schemes as a function of the allowed latency τ . Note that the energy consumption is the same for both NoOpt (yellow curve) and Blind-NoDFS (black curve).



(b) Breakdown of the energy consumed by the three phases of the collaboration as a function of the allowed latency τ . Note that the energy consumption for the Reduce phase is the same for both NoDFS and Blind-NoDFS.

Fig. 8. Energy consumption of the devices when $L = 1$ Mb, $\beta L = 0.1$ kb and $N = 10$. Each point is the result of an average over 100 feasible (for each scheme) instances of the problem, i.e., instances for which $L \leq L_{\max}^{\text{Opt}}, L_{\max}^{\text{Blind}}$. Note that the parameters have also been chosen to allow comparison between the schemes, i.e., to ensure that feasible instances arise with reasonable probability for all schemes.

end devices is the primary objective, care should be taken to avoid simply ignoring the energy burden imposed to the edge of the network. On the other hand, the system could also optimize channel and bandwidth allocation across devices, considered to be given in this work. The Shuffle phase could also be further optimized by integrating results from CDC [17]–[22]. These additional degrees of freedom could enable additional energy savings and increased system-wise performance. This would however come at the cost of a complexified optimization problem, and a sweet spot between optimization complexity and efficiency gains should thus be found.

ACKNOWLEDGMENT

AP is a Research Fellow of the F.R.S.-FNRS. This work was also supported by F.R.S.-FNRS under the EOS program (project 30452698, “MUlti-SERvice WIreless NETwork”). Authors would also like to thank our colleague Emre Kilcioglu for proofreading and comments, and the anonymous reviewers for their constructive criticism.

APPENDIX

A. Proof of Lemma 3

Problem (15) being convex, the optimal solution satisfies the KKT conditions. The Lagrangian of problem (15) is given by

$$\begin{aligned} \mathcal{L}_{1,n} = & \frac{\kappa_n c_n^3 l_n^3}{(t_n^{\text{MAP}})^2} + (\alpha \mu_n - \lambda) l_n + \beta_n t_n^{\text{MAP}} - \gamma_{1,n} l_n \\ & + \gamma_{2,n} \left(l_n - \frac{t_n^{\text{MAP}} f_n^{\text{max}}}{c_n} \right) - \gamma_{3,n} t_n^{\text{MAP}} + \gamma_{4,n} (t_n^{\text{MAP}} - \tau) \end{aligned}$$

with $\gamma_{1,n}, \gamma_{2,n}, \gamma_{3,n}, \gamma_{4,n} \geq 0$ the Lagrange multipliers. The KKT conditions are then given by

$$\frac{\partial \mathcal{L}_{1,n}}{\partial l_n} = 3 \frac{\kappa_n c_n^3 l_n^2}{(t_n^{\text{MAP}})^2} + \alpha \mu_n - \lambda - \gamma_{1,n} + \gamma_{2,n} = 0 \quad (27)$$

$$\frac{\partial \mathcal{L}_{1,n}}{\partial t_n^{\text{MAP}}} = -2 \frac{\kappa_n c_n^3 l_n^3}{(t_n^{\text{MAP}})^3} + \beta_n - \gamma_{2,n} \frac{f_n^{\text{max}}}{c_n} - \gamma_{3,n} + \gamma_{4,n} = 0 \quad (28)$$

with the complementary slackness conditions

$$\gamma_{1,n} l_n = 0, \quad (29)$$

$$\gamma_{2,n} \left(l_n - \frac{t_n^{\text{MAP}} f_n^{\text{max}}}{c_n} \right) = 0, \quad (30)$$

$$\gamma_{3,n} t_n^{\text{MAP}} = 0, \quad (31)$$

$$\gamma_{4,n} (t_n^{\text{MAP}} - \tau) = 0. \quad (32)$$

We first obtain (18), (19) and (21) using condition (27) and complementary slackness conditions (29) and (30). Substituting (18) in (28) and defining $\rho_{1,n} = \gamma_{4,n} - \gamma_{3,n}$, we then obtain (20) using complementary slackness conditions (31) and (32).

B. Proof of Lemma 4

Problem (16) being convex, the optimal solution satisfies the KKT conditions. The Lagrangian of problem (16) is given by

$$\begin{aligned} \mathcal{L}_{2,n} = & E_n + t_n^{\text{SHU}} P_n^c - \mu_n t_n^{\text{SHU}} r_n \left(\frac{E_n}{t_n^{\text{SHU}}} \right) + \beta_n t_n^{\text{SHU}} - \delta_{1,n} E_n \\ & + \delta_{2,n} (E_n - t_n^{\text{SHU}} p_n^{\text{max}}) - \delta_{3,n} t_n^{\text{SHU}} + \delta_{4,n} (t_n^{\text{SHU}} - \tau) \end{aligned}$$

with $\delta_{1,n}, \delta_{2,n}, \delta_{3,n}, \delta_{4,n} \geq 0$ the Lagrange multipliers. The KKT conditions are then given by

$$\frac{\partial \mathcal{L}_{2,n}}{\partial E_n} = 1 - \delta_{1,n} + \delta_{2,n} - \mu_n \frac{\frac{h_n}{N_0}}{1 + \frac{E_n}{t_n^{\text{SHU}}} \frac{h_n}{BN_0}} = 0 \quad (33)$$

$$\frac{\partial \mathcal{L}_{2,n}}{\partial t_n^{\text{SHU}}} = \mu_n \frac{\frac{E_n}{t_n^{\text{SHU}}} \frac{h_n}{N_0}}{1 + \frac{E_n}{t_n^{\text{SHU}}} \frac{h_n}{BN_0}} - \mu_n r_n \left(\frac{E_n}{t_n^{\text{SHU}}} \right) + P_n^c + \beta_n - \delta_{2,n} p_n^{\text{max}} - \delta_{3,n} + \delta_{4,n} = 0 \quad (34)$$

with the complementary slack conditions

$$\delta_{1,n} E_n = 0 \quad (35)$$

$$\delta_{2,n} (E_n - t_n^{\text{SHU}} p_n^{\text{max}}) = 0 \quad (36)$$

$$\delta_{3,n} t_n^{\text{SHU}} = 0 \quad (37)$$

$$\delta_{4,n} (t_n^{\text{SHU}} - \tau) = 0. \quad (38)$$

We first obtain (22), (23) and (25) using condition (33) and complementary slackness conditions (35) and (36). Substituting (22) in (34) and defining $\rho_{2,n} = \delta_{4,n} - \delta_{3,n}$, we then obtain (24) using complementary slackness conditions (37) and (38).

C. Proof of Lemma 5

Problem (17) being convex, the optimal solution satisfies the KKT conditions. The Lagrangian of problem (17) is given by

$$\mathcal{L}_3 = \sum_{n=1}^N \frac{\kappa_n c_n^3 T^3}{(t^{\text{RED}})^2} + \beta_n t^{\text{RED}} + \epsilon_1 \left(\max_n \left\{ \frac{c_n \beta L}{f_n^{\text{max}}} \right\} - t^{\text{RED}} \right) + \epsilon_2 (t^{\text{RED}} - \tau)$$

with $\epsilon_1, \epsilon_2 \geq 0$ the Lagrange multipliers. The KKT conditions are then given by

$$\frac{\partial \mathcal{L}_3}{\partial t^{\text{RED}}} = \epsilon_2 - \epsilon_1 - 2 \left(\frac{T}{t^{\text{RED}}} \right)^3 \sum_{n=1}^N \kappa_n c_n^3 + \sum_{n=1}^N \beta_n = 0 \quad (39)$$

with the complementary slackness conditions

$$\epsilon_1 \left(\max_n \left\{ \frac{c_n \beta L}{f_n^{\max}} \right\} - t^{\text{RED}} \right) = 0 \quad (40)$$

$$\epsilon_2 (t^{\text{RED}} - \tau) = 0. \quad (41)$$

Condition (39) together with complementary slackness conditions (40) (41) allow us to obtain (26).

REFERENCES

- [1] M. Chiang and T. Zhang, "Fog and IoT: An Overview of Research Opportunities," *IEEE Internet of Things Journal*, vol. 3, no. 6, pp. 854–864, Dec 2016.
- [2] A. Mammela and A. Anttonen, "Why Will Computing Power Need Particular Attention in Future Wireless Devices?" *IEEE Circuits and Systems Magazine*, vol. 17, no. 1, pp. 12–26, Firstquarter 2017.
- [3] S. Barbarossa, S. Sardellitti, and P. Di Lorenzo, "Communicating While Computing: Distributed mobile cloud computing over 5G heterogeneous networks," *IEEE Signal Processing Magazine*, vol. 31, no. 6, pp. 45–55, Nov 2014.
- [4] H. T. Dinh, C. Lee, D. Niyato, and P. Wang, "A survey of mobile cloud computing: architecture, applications, and approaches," *Wireless Communications and Mobile Computing*, vol. 13, no. 18, pp. 1587–1611, 2013.
- [5] Y. C. Hu, M. Patel, D. Sabella, N. Sprecher, and V. Young, "Mobile Edge Computing - A key technology towards 5G," *ETSI white paper*, vol. 11, no. 11, pp. 1–16, 2015.
- [6] Y. Mao, C. You, J. Zhang, K. Huang, and K. B. Letaief, "A Survey on Mobile Edge Computing: The Communication Perspective," *IEEE Communications Surveys Tutorials*, vol. 19, no. 4, pp. 2322–2358, Fourthquarter 2017.
- [7] P. Mach and Z. Becvar, "Mobile Edge Computing: A Survey on Architecture and Computation Offloading," *IEEE Communications Surveys Tutorials*, vol. 19, no. 3, pp. 1628–1656, thirdquarter 2017.
- [8] L. M. Vaquero and L. Rodero-Merino, "Finding Your Way in the Fog: Towards a Comprehensive Definition of Fog Computing," *SIGCOMM Comput. Commun. Rev.*, vol. 44, no. 5, p. 27–32, Oct. 2014.
- [9] Y. Shi, K. Yang, T. Jiang, J. Zhang, and K. B. Letaief, "Communication-Efficient Edge AI: Algorithms and Systems," *IEEE Communications Surveys and Tutorials*, 2020.
- [10] E. El Haber, T. M. Nguyen, and C. Assi, "Joint Optimization of Computational Cost and Devices Energy for Task Offloading in Multi-Tier Edge-Clouds," *IEEE Transactions on Communications*, vol. 67, no. 5, pp. 3407–3421, May 2019.
- [11] C. Zhang, P. Patras, and H. Haddadi, "Deep Learning in Mobile and Wireless Networking: A Survey," *IEEE Communications Surveys and Tutorials*, vol. 21, no. 3, pp. 2224–2287, 2019.
- [12] R. Stahl, Z. Zhao, D. Mueller-Gritschneider, A. Gerstlauer, and U. Schlichtmann, "Fully Distributed Deep Learning Inference on Resource-Constrained Edge Devices," in *Embedded Computer Systems: Architectures, Modeling, and Simulation*, D. N. Pnevmatikatos, M. Pelcat, and M. Jung, Eds. Cham: Springer International Publishing, 2019, pp. 77–90.
- [13] N. D. Lane, S. Bhattacharya, A. Mathur, P. Georgiev, C. Forlivesi, and F. Kawsar, "Squeezing Deep Learning into Mobile and Embedded Devices," *IEEE Pervasive Computing*, vol. 16, no. 3, pp. 82–88, 2017.
- [14] K. B. Letaief, W. Chen, Y. Shi, J. Zhang, and Y. A. Zhang, "The Roadmap to 6G: AI Empowered Wireless Networks," *IEEE Communications Magazine*, vol. 57, no. 8, pp. 84–90, 2019.

- [15] J. Park, S. Samarakoon, A. Elgabli, J. Kim, M. Bennis, S.-L. Kim, and M. Debbah, "Communication-Efficient and Distributed Learning Over Wireless Networks: Principles and Applications," *arXiv*, no. 2008.02608, 2020.
- [16] A. Paris, H. Mirghasemi, I. Stupia, and L. Vandendorpe, "Energy-Efficient Edge-Facilitated Wireless Collaborative Computing using Map-Reduce," in *2019 IEEE 20th International Workshop on Signal Processing Advances in Wireless Communications (SPAWC)*, July 2019, pp. 1–5.
- [17] S. Li, Q. Yu, M. A. Maddah-Ali, and A. S. Avestimehr, "A Scalable Framework for Wireless Distributed Computing," *IEEE/ACM Transactions on Networking*, vol. 25, no. 5, pp. 2643–2654, Oct 2017.
- [18] M. Kiamari, C. Wang, and A. S. Avestimehr, "Coding for Edge-Facilitated Wireless Distributed Computing with Heterogeneous Users," in *2017 51st Asilomar Conference on Signals, Systems, and Computers*, Oct 2017, pp. 536–540.
- [19] S. Li, M. A. Maddah-Ali, Q. Yu, and A. S. Avestimehr, "A Fundamental Tradeoff Between Computation and Communication in Distributed Computing," *IEEE Transactions on Information Theory*, vol. 64, no. 1, pp. 109–128, Jan 2018.
- [20] F. Li, J. Chen, and Z. Wang, "Wireless MapReduce Distributed Computing," *arXiv*, no. 1802.00894, 2018.
- [21] S. Li, M. A. Maddah-Ali, and A. S. Avestimehr, "Coding for Distributed Fog Computing," *IEEE Communications Magazine*, vol. 55, no. 4, pp. 34–40, 2017.
- [22] F. Xu and M. Tao, "Heterogeneous Coded Distributed Computing: Joint Design of File Allocation and Function Assignment," *2019 IEEE Global Communications Conference (GLOBECOM)*, Dec 2019.
- [23] J. Dean and S. Ghemawat, "MapReduce: Simplified Data Processing on Large Clusters," in *OSDI'04: Sixth Symposium on Operating System Design and Implementation*, San Francisco, CA, 2004, pp. 137–150.
- [24] X. Cao, F. Wang, J. Xu, R. Zhang, and S. Cui, "Joint Computation and Communication Cooperation for Energy-Efficient Mobile Edge Computing," *IEEE Internet of Things Journal*, vol. 6, no. 3, pp. 4188–4200, June 2019.
- [25] C. You and K. Huang, "Exploiting Non-Causal CPU-State Information for Energy-Efficient Mobile Cooperative Computing," *IEEE Transactions on Wireless Communications*, vol. 17, no. 6, pp. 4104–4117, June 2018.
- [26] Z. Sheng, C. Mahapatra, V. C. M. Leung, M. Chen, and P. K. Sahu, "Energy Efficient Cooperative Computing in Mobile Wireless Sensor Networks," *IEEE Transactions on Cloud Computing*, vol. 6, no. 1, pp. 114–126, Jan 2018.
- [27] D. Wu, F. Wang, X. Cao, and J. Xu, "Wireless Powered User Cooperative Computation in Mobile Edge Computing Systems," *arXiv*, no. 1809.01430, 2018.
- [28] A. Mtibaa, A. Fahim, K. A. Harras, and M. H. Ammar, "Towards Resource Sharing in Mobile Device Clouds: Power Balancing across Mobile Devices," *SIGCOMM Comput. Commun. Rev.*, vol. 43, no. 4, p. 51–56, Aug. 2013.
- [29] L. Pu, X. Chen, J. Xu, and X. Fu, "D2D Fogging: An Energy-Efficient and Incentive-Aware Task Offloading Framework via Network-assisted D2D Collaboration," *IEEE Journal on Selected Areas in Communications*, vol. 34, no. 12, pp. 3887–3901, Dec 2016.
- [30] K. Yang, Y. Shi, and Z. Ding, "Low-rank optimization for data shuffling in wireless distributed computing," in *2018 IEEE International Conference on Acoustics, Speech and Signal Processing (ICASSP)*, 04 2018, pp. 6343–6347.
- [31] M. S. Andersen, J. Dahl, and L. Vandenberghe, "CVXOPT: A Python package for convex optimization." [Online]. Available: <https://cvxopt.org/>